Performance Evaluation of ITLinQ and FlashLinQ for Overlaid Device-to-Device Communication

Ratheesh K. Mungara*, Xinchen Zhang†, Angel Lozano*, and Robert W. Heath, Jr.‡
* Universitat Pompeu Fabra (UPF), Barcelona, Spain
† Qulacomm Inc., San Diego, CA 92121, USA
‡ The University of Texas at Austin, Austin, TX, USA
Emails: {ratheesh.mungara, angel.lozano}@upf.edu, {x.zhang, rheath}@utexas.edu

***Abstract*—We present a performance evaluation of ITLinQ and FlashLinQ, the two most popular schemes proposed to date to *channelize* D2D transmissions, i.e., to parse transmissions into noninterfering sets to be allocated to separate channels. Recognizing that it captures well the spatial characteristics of D2D networks, a stochastic geometry setting is utilized for this evaluation with the parameters of either scheme optimized in order to maximize the system spectral efficiency (bits/s/Hz per unit area). Although independently formulated and seemingly based on different principles, both schemes are found to exercise similar mechanisms to avoid situations of excessive interference, yielding substantial improvements with respect to unchannelized networks.**

I. Introduction

The overlay of D2D communication onto infrastructure-based wireless networks promises major performance advantages provided there is sufficient locality in the traffic [1]–[6]. Without a careful assignment of D2D links to time/frequency signaling channels, which we shorted as *channelization*, a significant share of the D2D links may experience strong interference from nearby unintended transmissions and, as the density increases, this interference may progressively clog the network.

This issue can be mitigated by channelizing in a way that prevents situations of excessive interference. Schemes aimed at doing that had been studied in the context of wireless ad-hoc networks, where fixed infrastructure is absent [7]–[12]; with the growing interest in overlaid D2D, new schemes are being discussed that can suit networks with an infrastructure-supported control plane and the ensuing ability to synchronize, discover neighbors, and disseminate side information:

1) A first such scheme, termed FlashLinQ, was formulated in [13], [14] and experimentally demonstrated.
2) A subsequent scheme, inspired by information-theoretic optimality notions and referred to as ITLinQ, was proposed in [15]. Its performance was quantified through Monte-Carlo simulations.

A stochastic-geometry-based analytical characterization of ITLinQ was put forth in [16], advancing its understanding and offering a complement to Monte-Carlo simulations, but falling short of establishing its benefits over FlashLinQ. The goal of the present paper is to establish these benefits—particularly in terms of system spectral efficiency—and to shed light on the mechanisms that each scheme utilizes to shield users from excessive interference while attempting to pack as many concurrent D2D transmissions per unit area as possible.

This work was supported in part by Intel's University Research Program "5G: Transforming the Wireless User Experience", by the MINECO Project TEC2012-34642 and by the National Science Foundation Grant No. 1218338.

II. System Model

Recognizing that a stochastic geometry toolbox allows for models that are both amenable to analytical treatment and highly representative of the spatial behavior of D2D users, this is the approach taken for our performance evaluation. This section lays down the specific models utilized in the sequel.

A. User Spatial Distribution

We consider the Poisson bipolar model [17] where D2D transmitters are spatially distributed according to a marked[1] homogeneous PPP $\hat{\Phi} = \{(x_k, \theta_k, m_k, e_k)\} \subset \mathbb{R}^2 \times [0, 2\pi) \times [0, 1] \times \{0, 1\}$ where:

- $\Phi = \{x_k\} \subset \mathbb{R}^2$ is the uniform PPP with intensity λ representing the locations of all existing transmitters with x_k the location of the kth-link transmitter.
- θ_k denotes the IID (independent identically distributed) orientation angle, uniformly distributed in $[0, 2\pi)$, between the transmitter at x_k and its intended receiver.
- m_k is an IID random mark associated with the kth link, uniformly distributed in $[0, 1]$, which may represent the time stamp or the priority of the kth link.
- $e_k \in \{0, 1\}$ is a retaining indicator that indicates whether the kth-link is allowed on a given channel.

Denoting by r_{v_k,x_k} the distance between the kth-link transmitter and its intended receiver, the location of the latter is $v_k = x_k + [r_{v_k,x_k} \cos\theta_k, r_{v_k,x_k} \sin\theta_k]^T$. In the absence of empirical data on how r_{v_k,x_k} is distributed, various canonical distributions have been entertained in the literature including Rayleigh distributions [18], [19], inverse functions of the link density [15], [20], or a uniform distribution within a circle

[1] A marked PPP is a Poisson point process where each point is labeled with a mark, whose distribution features additional information such as transmit power, fading, or priority of the link.

centered on the transmitter [21]. Alternatively, we consider the flexible discrete marginal distribution (IID across links)

$$r_{v_k,x_k} = d_n \quad \text{with probability} \quad p_n \tag{1}$$

and with $\sum_{n=1}^{N} p_n = 1$. By choosing N and the appropriate values for $d_1, \ldots, d_N$ and $p_1, \ldots, p_N$, we can reproduce as approximately as desired the behavior of any of the aforementioned continuous distributions.

B. Signal Model

By Slivnyak's Theorem [22], we can place at the origin a receiver and center the analysis on its link, indexed by 0. This link, whose transmitter is located at x_0, can serve as the typical link in the network.

Denoting by P the signal power measured at 1 m from its transmitter, the receiver at the origin observes

$$y_0 = \sqrt{P\, r_{v_0,x_0}^{-\eta}}\, h_{v_0,x_0} s_0 + z_0' \tag{2}$$

where the first term is the intended signal while the second term is the aggregate interference plus noise

$$z_0' = \sum_{k=1}^{\infty} \sqrt{P\, r_{v_0,x_k}^{-\eta}}\, e_k\, h_{v_0,x_k} s_k + z_0 \tag{3}$$

where the summation spans the co-channel transmitters in $\Phi \setminus \{x_0\}$ while z_0 denotes the AWGN. In turn, $\eta > 2$ is the pathloss exponent, r_{v_0,x_k} is the distance between v_0 and x_k (i.e., from the transmitter at x_k to the receiver at v_0), h_{v_0,x_k} denotes the corresponding fading, and s_k is the data symbol communicated over the kth link. The fading coefficient h_{v_0,x_k} is IID complex Gaussian with zero mean and unit variance, i.e., $h_{v_0,x_k} \sim \mathcal{N}_{\mathbb{C}}(0,1)$. Likewise, $s_k \sim \mathcal{N}_{\mathbb{C}}(0,1)$ and $z_0 \sim \mathcal{N}_{\mathbb{C}}(0, N_0 B)$ where N_0 is the noise power spectral density and B is the bandwidth.

The local-average SNR (signal-to-noise ratio) at the 0th-link receiver is

$$\mathsf{SNR} = \frac{P}{N_0 B}\, r_{v_0,x_0}^{-\eta}. \tag{4}$$

Shadow fading, not considered here, could possibly be incorporated by adopting the approach in [23]. Shadow fading can be seen as a distortion of the spatial geometry, something that in our case would render any circular region amorphous and modify the quantitative results but would otherwise preserve the intuition and the qualitative assesments.

III. ITLinQ

A. Description

ITLinQ is grounded on a certain information-theoretic optimality notion: it selects, for each channel, a subset of links whose mutual interference can be treated as noise while still achieving the capacity region of that subset to within a constant gap [15]. That amounts to assigning the 0th link to a channel if and only if its transmitter and receiver satisfy the necessary and sufficient condition

$$\mathsf{SNR} \geq \max_{k \neq 0} \mathsf{INR}_{0,k}^{\text{in}} \max_{i \neq 0} \mathsf{INR}_{i,0}^{\text{out}} \tag{5}$$

where $\mathsf{INR}_{0,k}^{\text{in}}$ is the incoming local-average INR (interference-to-noise ratio) from link k to link 0, i.e., the INR from the kth-link transmitter to the 0th-link receiver, given by

$$\mathsf{INR}_{0,k}^{\text{in}} = \frac{P}{N_0 B}\, r_{v_0,x_k}^{-\eta} \tag{6}$$

while $\mathsf{INR}_{i,0}^{\text{out}}$ is the outgoing local-average INR to link i from link 0, i.e., the INR from the 0th-link transmitter to the ith-link receiver

$$\mathsf{INR}_{i,0}^{\text{out}} = \frac{P}{N_0 B}\, r_{v_i,x_0}^{-\eta}. \tag{7}$$

To implement (5), a centralized controller having local-average channel knowledge of all the links would be required. To relax this requirement, a distributed version of ITLinQ was proposed in [15, Sec. III] where each transceiver can check its own condition locally with respect to already retained links, sequentially. This distributed version of ITLinQ relies only on two sufficient conditions, derived from (5), which expressed for the 0th link amount to

$$\mathsf{SNR}^{1/2} \geq \max_{k \neq 0} \mathsf{INR}_{0,k}^{\text{in}} \tag{8}$$

$$\mathsf{SNR}^{1/2} \geq \max_{i \neq 0} \mathsf{INR}_{i,0}^{\text{out}} \tag{9}$$

where (8) must be satisfied at the receiver of link 0 while (9) must be satisfied at the corresponding transmitter. Because distributed ITLinQ is based on sufficient but not necessary conditions, it is overly conservative and hence it experiences a certain loss relative to centralized ITLinQ. This loss can be eliminated almost completely by heuristically modifying the sufficient conditions in (8) and (9) into [15]

$$M \mathsf{SNR}^{\mu} \geq \mathsf{INR}_{0,k}^{\text{in}} \qquad \forall k \neq 0 \tag{10}$$

$$M \mathsf{SNR}^{\mu} \geq \mathsf{INR}_{i,0}^{\text{out}} \qquad \forall i \neq 0 \tag{11}$$

where M and μ are positive parameters.

A slightly different distributed form of ITLinQ is considered here, inspired by the Matérn hard-core processes of type II that is widely utilized to analyze CSMA [9], [12]. In this ITLinQ type II, the sequentiality in the application of the conditions is replaced by a prioritization embodied by the marks m_k. Rather than against previous links, the conditions are verified against lower-priority links, i.e., the links are prioritized by the network and the 0th link is allowed in a channel if and only if conditions (10) and (11) are satisfied with respect to the subset of transmitters or receivers with lower mark, $i, k \in \{n : m_n < m_0\}$. If not allowed in a given channel, then the 0th link is served on another channel and thus we can regard the analysis as corresponding to the channel where this link is served.

B. Geometric Interpretation

Plugging into the condition in (10) the definitions of SNR and $\mathsf{INR}_{0,k}^{\text{in}}$ given in (4) and (6), respectively, we obtain

$$r_{v_0 x_k} \geq \frac{r_{v_0 x_0}^{\mu}}{M^{1/\eta}} \left(\frac{P}{N_0 B} \right)^{\frac{1-\mu}{\eta}} \tag{12}$$

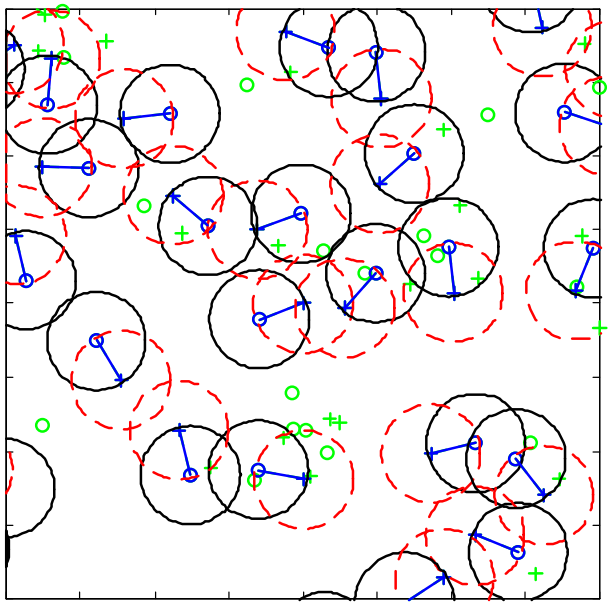

Fig. 1: Channelized network realization under ITLinQ. Transmitters and receivers are indicated by $\circ$ and $+$, respectively. Links allowed to coexist on the channel of interest are connected by solid lines while other links are not connected. Solid and dashed circles represent the exclusion regions around transmitters and receivers, respectively. In this example, every link has the same distance and hence all exclusion regions are equally sized.

leading to the equivalent condition

$$r_{v_0 x_k} \geq \mathsf{r} \tag{13}$$

with

$$\mathsf{r} = \frac{r_{v_0,x_0}^{\mu}}{M^{1/\eta}} \left(\frac{P}{N_0 B} \right)^{\frac{1-\mu}{\eta}} \tag{14}$$

Thus, ITLinQ surrounds the receivers with exclusion regions of radius r where no lower-priority transmitters are present.

Likewise, by plugging (4) and (7) into (11), it can be verified that ITLinQ surrounds the transmitters with exclusion regions of radius r where no lower-priority receivers are present.

All these exclusion regions, illustrated in Fig. 1, curb interference from lower-priority links and ensure that conditions (10) and (11) are satisfied as far as those links are concerned.

C. Co-Channel Link Density

Next, we characterize the density of links that end up coexisting on a given channel when ITLinQ type II is applied.

On the channel serving the 0th link, the network that results is indicated by $\hat{\Psi}_{\mathrm{II}} = \{(x_k, \theta_k) : (x_k, \theta_k, m_k, e_k) \in \hat{\Phi} \text{ and } e_k = 1\}$ while the process of co-channel transmitter locations is represented by $\Psi_{\mathrm{II}} = \{x_k : (x_k, \theta_k) \in \hat{\Psi}_{\mathrm{II}}\}$.

Let $\mathcal{B}_x(\mathsf{r})$ denote a circle centered at x with radius r and let $\mathbb{1}(\cdot)$ be the indicator function returning 1 if its argument is true and 0 otherwise.

Lemma 1. *The co-channel link density of ITLinQ type II is*

$$\lambda_{\Psi_{\mathrm{II}}} = \sum_{n=1}^{N} \frac{p_n}{A(\mathsf{r}_n, d_\ell)} \left(1 - e^{-\lambda A(\mathsf{r}_n, d_\ell)} \right) \tag{15}$$

where r_n is the exclusion region radius corresponding to $r_{v_0,x_0} = d_n$ in (14) while

$$A(\mathsf{r}_n, d_\ell) = \pi \mathsf{r}_n^2 + \sum_{\ell=1}^{N} p_\ell \int \left(1 - \mathbb{P}\left(v_i \notin \mathcal{B}_{x_0}(\mathsf{r}_n) | x_i, r_{v_i,x_i} = d_\ell \right) \right) \mathrm{d}x_i$$

with integration over $\mathcal{B}_{x_0}(\mathsf{r}_n + d_\ell) \setminus \mathcal{B}_{v_0}(\mathsf{r}_n)$ and with

$$\mathbb{P}\left(v_i \notin \mathcal{B}_{x_0}(\mathsf{r}_n) | x_i, r_{v_i,x_i} = d_\ell \right) = \begin{cases} \mathbb{1}(\mathsf{r}_n < d_\ell) & 0 \leq r_{x_i,x_0} \leq |\mathsf{r}_n - d_\ell| \\ 1 - \frac{\arccos\left(\frac{r_{x_i,x_0}^2 + d_\ell^2 - \mathsf{r}_n^2}{2\, r_{x_i,x_0}\, d_\ell} \right)}{\pi} & |\mathsf{r}_n - d_\ell| < r_{x_i,x_0} \leq \mathsf{r}_n + d_\ell \\ 1 & r_{x_i,x_0} > \mathsf{r}_n + d_\ell \end{cases}$$

the probability that the receiver of the ith link is not in $\mathcal{B}_{x_0}(\mathsf{r}_n)$ conditioned on the location of the ith-link transmitter x_i.

Proof. See [24]. □

D. Average Spectral Efficiency

Because of the dependent thinning that ITLinQ effects on the initial PPP Φ, the process of co-channel transmitter locations Ψ_{II} is no longer a PPP. To circumvent the analytical obstacle that this represents, we adopt a modelling assumption introduced in [8] and whose goodness is validated in [16] and later in this very paper: the locations of co-channel transmitters *outside* the receiver's exclusion region belong to a homogeneous PPP with the density $\lambda_{\Psi_{\mathrm{II}}}$ that we derived in Lemma 1. Under these conditions, the ensuing proposition generalizes the fixed-link-distance result in [16, Prop. 1].

Proposition 1. *For transmitter density λ and parameters M and μ, the spatially averaged link spectral efficiency (b/s/Hz per link) of ITLinQ type II equals*

$$\bar{C}(\lambda, M, \mu) = \sum_{n=1}^{N} q_n \int_0^{\infty} \frac{\log_2 e}{\gamma + 1} \exp\left\{ -\frac{\gamma}{d_n^{-\eta}} \frac{N_0 B}{P} + \pi \lambda_{\Psi_{\mathrm{II}}} \mathsf{r}_n^2 + \frac{2}{\eta} \pi \lambda_{\Psi_{\mathrm{II}}} \gamma^{\frac{2}{\eta}} d_n^2\, \bar{\Gamma}\left(-\frac{2}{\eta}, \gamma \left(\frac{d_n}{\mathsf{r}_n} \right)^{\eta} \right) \right\} \mathrm{d}\gamma$$

where q_n is the fraction of co-channel links with link distance d_n and $\lambda_{\Psi_{\mathrm{II}}}$ is given by (15).

Proof. See [24]. □

From Prop. 1, the spatially averaged system spectral efficiency (b/s/Hz per unit area) can be obtained by scaling the

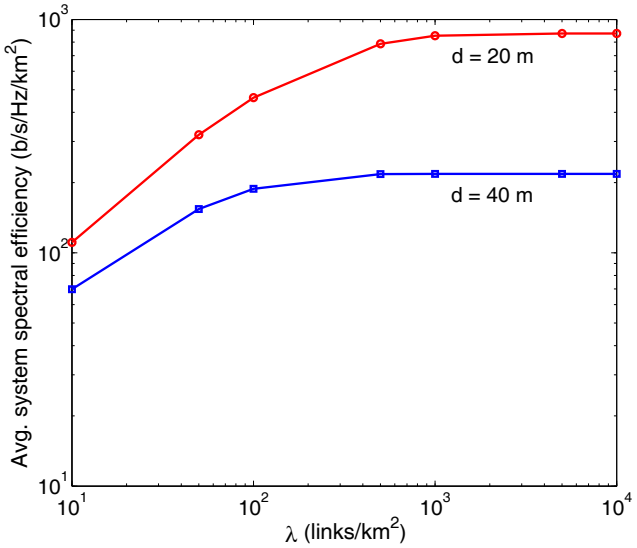

Fig. 2: Average system spectral efficiency v. λ for optimized ITLinQ type II with $d = 20$ m and $d = 40$ m, and with $\eta = 4.5$ and $\frac{P}{N_0 B} = 117$ dB.

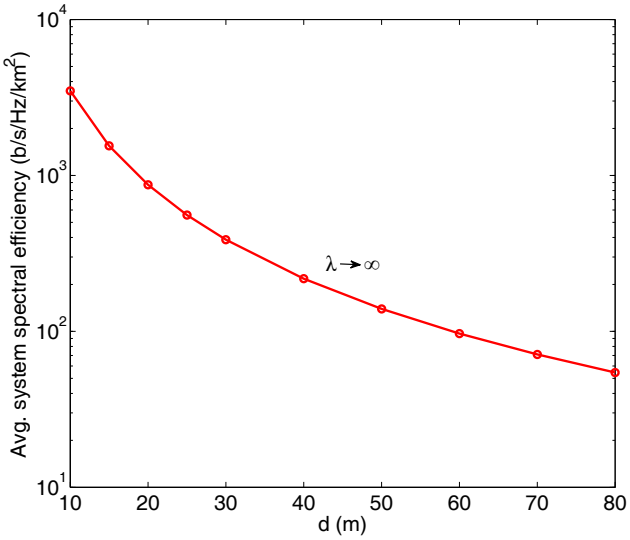

Fig. 3: Average system spectral efficiency v. d for optimized ITLinQ type II with $\lambda \to \infty$, $\eta = 4.5$ and $\frac{P}{N_0 B} = 117$ dB.

spatially averaged link spectral efficiency by the co-channel link density, $\lambda_{\Psi_{\rm II}}$, giving

$$\bar{\mathcal{C}}(\lambda, M, \mu) = \lambda_{\Psi_{\rm II}} \bar{C}(\lambda, M, \mu). \tag{16}$$

Finally, the parameters M and μ can be tuned as function of the user density and link distance distribution in order to maximize the average system spectral efficiency, i.e., to obtain

$$\bar{\mathcal{C}}^\star(\lambda) = \max_{M>0, \mu>0} \bar{\mathcal{C}}(\lambda, M, \mu) \tag{17}$$

Example 1. Shown in Fig. 2 is the average system spectral efficiency of ITLinQ type II obtained by numerically solving (17) with link distances fixed at either $d = 20$ m or $d = 40$ m. The limiting ($\lambda \to \infty$) system spectral efficiency is presented in Fig. 3 as function of the link distance d, fixed for all users.

For any given link distance, the co-channel link density $\lambda_{\Psi_{\rm II}}$ increases with growing λ and eventually saturates. This, in turn, leads to saturation in the average system spectral efficiency.

IV. FlashLinQ

A. Description

In contrast with ITLinQ, whose channelization conditions are grounded in an information-theoretic optimality notion and then heuristically refined, FlashLinQ's channelization policy was formulated on a heuristic basis from the onset.

For the sake of consistency, and to ensure a fair comparison later, we consider a type II embodiment of FlashLinQ for which the 0th link is allowed in a channel if and only if two distinct conditions are satisfied with respect to links with a lower mark. The first condition is

$$\frac{\mathsf{SNR}}{\mathsf{INR}^{\rm out}_{i,0}} \geq \gamma_{\rm TX} \quad i \in \{n : m_n < m_0\} \tag{18}$$

which ensures that the outgoing interference caused by the 0th-link transmitter to lower-mark receiver is within a specified limit determined by the threshold $\gamma_{\rm TX}$; if (18) is not satisfied, then the 0th-link transmitter must *yield*, meaning that it must refrain from transmitting and thus the link must be allocated to another channel. In turn, the second condition is

$$\frac{\mathsf{SNR}}{\sum_k \mathsf{INR}^{\rm in}_{0,k}} \geq \gamma_{\rm RX} \quad k \in \{n : m_n < m_0\} \tag{19}$$

where $\gamma_{\rm RX}$ is an additional threshold; if (19) is not satisfied, then the 0th-link receiver must yield, meaning again that the link must be allocated to another channel.

B. Geometric Interpretation

Paraphrasing [14], the condition in (18) intends for the 0th link not to cause *too much interference* to other lower-mark links assigned to the channel under consideration. However, no specific SIR can be guaranteed for those other links as the condition limits the interference contribution of the 0th link without regard to how much other interference is present. Plugging into (18) the definitions of SNR and $\mathsf{INR}^{\rm out}_{i,0}$ given in (4) and (7), respectively, we obtain for the ith lower-mark interfered link the equivalent condition

$$r_{v_i,x_0} \geq r_{v_0,x_0}\, \gamma_{\rm TX}^{1/\eta} \tag{20}$$

whose enforcement amounts to forming around the transmitter a circular exclusion region that is free of any lower-mark receiver and whose radius is

$$r_{v_0,x_0}\, \gamma_{\rm TX}^{1/\eta}. \tag{21}$$

Contrasting this definition with ITLinQ's exclusion radius r (cf. Eq. 14), we observe that the two coincide if $\mu = 1$ and $M = 1/\gamma_{\rm TX}$.

Given that the first FlashLinQ condition by itself cannot prevent possible situations of excessive interference, it is reinforced by the second condition meant to help achieve, again paraphrasing [14], a *reasonable SIR* for the 0th link. Once more though, no specific value can be guaranteed for the SIR because the second condition too involves only links with lower marks; the interference from higher-mark links may push the SIR below γ_{RX} and, with some small probability, below even lower values. Furthermore, because the second condition involves not the interference from a specific link but a sum thereof, geometrically it amounts to forming an exclusion region that—even in the absence of shadowing—is not circular; this renders FlashLinQ's analysis rather unwieldy.

C. Average Spectral Efficiency

In the original formulation of FlashLinQ, fixed values were employed for γ_{TX} and γ_{RX} with the further restriction that $\gamma_{\mathrm{TX}} = \gamma_{\mathrm{RX}}$. Then, in [25], this restriction was lifted and the performance of FlashLinQ was numerically computed for varying threshold values to find that:

- The average system spectral efficiency decreases with growing γ_{TX}.
- The average system spectral efficiency increases with growing γ_{RX} for lower values of γ_{RX} and then gradually decreases with growing γ_{RX} for higher values of γ_{RX}.

V. Performance Evaluation

We can now proceed to evaluate the performance of ITLinQ and FlashLinQ with the respective parameters and thresholds optimized, producing more refined evaluations than the one in [15] where the ITLinQ parameters were optimized while the FlashLinQ thresholds were kept fixed to the default settings initially suggested in [13], [14].

Example 2. Fig. 4 shows, as function of λ, the average system spectral efficiency of optimized ITLinQ and FlashLinQ when every link has a distance of $d = 40$ m. Simulation results are shown for FlashLinQ whereas, for ITLinQ, both analytical and simulation results are available. And, as baseline, analytical and simulation results for the case that all links must coexist on a single channel are also included.

Example 3. Fig. 5 shows, as function of λ, the average system spectral efficiency of optimized ITLinQ and FlashLinQ when the link distances equiprobably take the values $d_1 = 20$ m, $d_2 = 40$ m, and $d_3 = 60$ m. Again, simulation results are shown for FlashLinQ and both analytical and simulation results for ITLinQ, and the no-channelization baseline results are included.

From the foregoing examples, we can draw the following observations:

- Despite the PPP approximation invoked in Section III-C, the analytical expressions derived for the spectral efficiency of ITLinQ are accurate—only slightly pessimistic—and offer an efficient alternative to simulations. Indeed, the generation of each optimized simulation point in Examples 2 and 3 is an extremely time-consuming process.
- As anticipated, both ITLinQ and FlashLinQ yield a significant improvement in average performance relative to unchannelized baseline, particularly in dense networks. (For links that are close-by, the improvement brought about by channelization is much more pronounced.)
- Surprisingly given its fully heuristic nature, if its thresh-

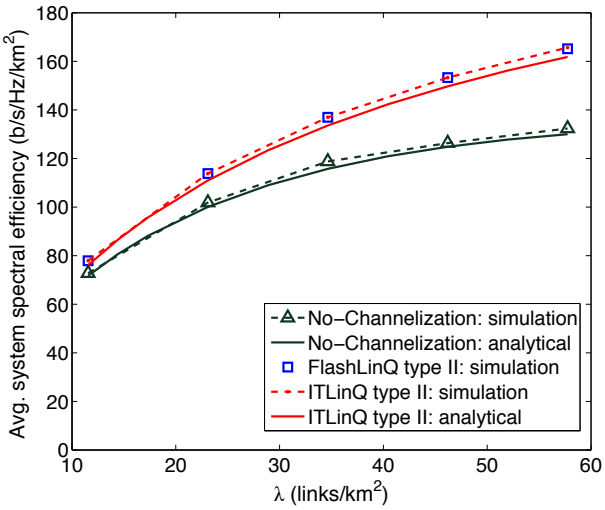

Fig. 4: Average system spectral efficiency v. λ for optimized ITLinQ and optimized FlashLinQ with fixed link distances $d = 40$ m, and with $\eta = 4.5$ and $\frac{P}{N_0 B} = 117$ dB.

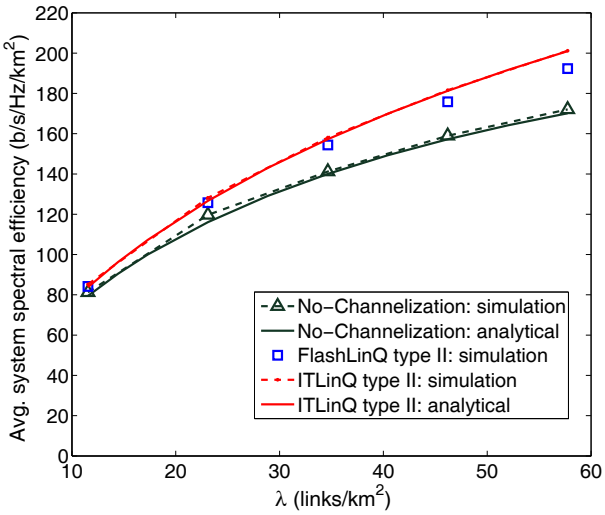

Fig. 5: Average system spectral efficiency v. λ for optimized ITLinQ and optimized FlashLinQ with randomized link distances (equiprobably $d_1 = 20$ m, $d_2 = 40$ m, and $d_3 = 60$ m), and with $\eta = 4.5$ and $\frac{P}{N_0 B} = 117$ dB.

olds are optimized FlashLinQ is essentially as effective as ITLinQ. In Example 2 their performance is identical and, in Example 3, they perform to within 5%.

The above observations have been verified to hold qualitatively for other link distance distributions, for pathloss exponents ranging between $\eta = 3$ and $\eta = 4.5$, for dual-slope pathloss functions [26], and even with shadow fading incorporated.

VI. Conclusion

The availability of multiple channels in D2D networks offers the possibility of parsing the pool of available links onto various sets in such a way that excessive interference is avoided. The two schemes proposed to date to exploit this possibility, FlashLinQ and ITLinQ, operate by enforcing—through various parameters and thresholds—exclusion regions around transmitters and receivers. Both are similarly effective, with a slight edge for ITLinQ, and hence the decision on which one to implement may be based on how well they fit a particular system.

References

[1] K. Doppler, M. Rinne, C. Wijting, C. B. Ribeiro, and K. Hugl, "Device-to-Device communication as an underlay to LTE-advanced networks," *IEEE Commun. Mag.*, vol. 47, no. 12, pp. 42–49, Dec. 2009.

[2] G. Fodor, E. Dahlman, G. Mildh, S. Parkvall, N. Reider, G. Miklós, and Z. Turányi, "Design aspects of network assisted device-to-device communications," *IEEE Commun. Mag.*, vol. 50, no. 3, pp. 170–177, Mar. 2012.

[3] L. Lei, Z. Zhong, C. Lin, and X. Shen, "Operator controlled device-to-device communications in LTE-advanced networks," *IEEE Trans. Wireless Commun.*, vol. 19, no. 3, pp. 96–104, June 2012.

[4] 3GPP TR 22.803 V1.0.0, "Feasibility Study for Proximity Services (ProSe) (Release 12)," Tech. Rep., 3rd Generation Partnership Project 3GPP, www.3gpp.org, Aug. 2012.

[5] F. Boccardi, R. W. Heath Jr., A. Lozano, T. Marzetta, and P. Popovski, "Five disruptive technology directions for 5G," *IEEE Commun. Mag.*, vol. 52, no. 2, pp. 74–80, Feb. 2014.

[6] J. G. Andrews, S. Buzzi, W. Choi, S. Hanly, A. Lozano, A. C. K. Soong, and J. C. Zhang, "What will 5G be?," *IEEE J. Select. Areas Commun.*, vol. 32, no. 6, pp. 1065–1082, June 2014.

[7] A. Hasan and J. Andrews, "The guard zone in wireless ad hoc networks," *IEEE Trans. Wireless Commun.*, vol. 6, no. 3, pp. 897–906, Mar. 2007.

[8] F. Baccelli, J. Li, T. Richardson, S. Shakkottai, S. Subramanian, and X. Wu, "On optimizing CSMA for wide area ad-hoc networks," in *Proc. Int. Symp. on Modelling and Opt. in Mobile, Ad-hoc and Wireless Networks*, May 2011, pp. 354–359.

[9] M. Haenggi, "Mean interference in hard-core wireless networks," *IEEE Commun. Lett.*, vol. 15, no. 8, pp. 792–794, Aug. 2011.

[10] D. Torrieri and M. C. Valenti, "Exclusion and guard zones in DS-CDMA Ad Hoc networks," *IEEE Trans. Commun.*, vol. 61, no. 6, pp. 2468–2476, June 2013.

[11] G. Alfano, M. Garetto, and E. Leonardi, "New directions into the stochastic geometry analysis of dense CSMA networks," *IEEE Trans. Mobile Comput.*, vol. 13, no. 2, pp. 324–336, Feb. 2014.

[12] Y. Zhong, W. Zhang, and M. Haenggi, "Stochastic analysis of the mean interference for the RTS/CTS mechanism," in *Proc. IEEE Int. Conf. Commun.*, June 2014, pp. 1996–2001.

[13] X. Wu, S. Tavildar, S. Shakkottai, T. Richardson, J. Li, R. Laroia, and A. Jovicic, "FlashLinQ: A synchronous distributed scheduler for peer-to-peer ad hoc networks," in *Proc. Annual Allerton Conf. Commun., Cont., Computing*, Sept. 2010, pp. 514–521.

[14] X. Wu, S. Tavildar, S. Shakkottai, T. Richardson, J. Li, R. Laroia, and A. Jovicic, "FlashLinQ: A synchronous distributed scheduler for peer-to-peer ad hoc networks," *IEEE/ACM Trans. Networking*, vol. 21, no. 4, pp. 1215–1228, Aug. 2013.

[15] N. Naderializadeh and A. S. Avestimehr, "ITLinQ: A new approach for spectrum sharing in device-to-device communication systems," *IEEE J. Select. Areas Commun.*, vol. 32, no. 6, pp. 1139–1151, June 2014.

[16] R. K. Mungara, X. Zhang, A. Lozano, and R. W. Heath Jr., "On the spatial spectral efficiency of ITLinQ," in *Proc. Annual Asilomar Conf. Signals, Syst., Comp.*, Nov. 2014.

[17] F. Baccelli, B. Blaszczyszyn, and P. Muhlethaler, "Stochastic analysis of spatial and opportunistic Aloha," *IEEE J. Select. Areas Commun.*, vol. 27, no. 7, pp. 1105–1119, Sept. 2009.

[18] F. Baccelli, J. Li, T. Richardson, S. Shakkottai, S. Subramanian, and X. Wu, "On optimizing CSMA for wide area ad-hoc networks," in *Proc. Int. Symp. on Modelling and Opt. in Mobile, Ad-hoc and Wireless Networks*, May 2011, pp. 354–359.

[19] X. Lin, J. G. Andrews, and A. Ghosh, "Spectrum sharing for device-to-device communication in cellular networks," *IEEE Trans. Wireless Commun.*, vol. 13, no. 12, pp. 6727–6740, Dec. 2014.

[20] G. George, R. K. Mungara, and A. Lozano, "An analytical framework for device-to-device communication in cellular networks," Available online: http://arxiv.org/abs/1407.2201/, 2014.

[21] N. Lee, F. Baccelli, and R. W. Heath Jr., "Spectral efficiency scaling laws in dense random wireless networks with multiple receive antennas," [Online]. Available: http://arxiv.org/abs/1410.7502, 2014.

[22] M. Haenggi, *Stochastic Geometry for Wireless Networks*, Cambridge Univ. Press, Cambridge, U. K., 2012.

[23] P. Madhusudhanan, J. G. Restrepo, Y. E. Liu, and T. X. Brown, "Carrier to Interference ratio analysis for the shotgun cellular system," in *Proc. IEEE Global Commun. Conf.*, Honolulu, USA, Nov. 2009, pp. 1–6.

[24] R. K. Mungara, X. Zhang, A. Lozano, and R. W. Heath Jr., "Analysis of ITLinQ: Channel allocation for Device-to-Device communication networks," http://www.dtic.upf.edu/~alozano/papers/channelization.pdf, 2014.

[25] H. Yoon, J. S. Kim, S. J. Bae, B. Choi, and M. Y. Chung, "Performance analysis of FlashLinQ with various yielding threshold values," in *Proc. Int. Conf. ICT Convergence*, Oct. 2012, pp. 477–478.

[26] X. Zhang and J. G. Andrews, "Downlink cellular network analysis with multi-slope path loss models," [Online]. Available: http://arxiv.org/abs/1408.0549, 2014.